Korean J. Chem. Eng., **31**(1), 120-124 (2014)
DOI: 10.1007/s11814-013-0199-0

pISSN: 0256-1115
eISSN: 1975-7220

Solvated behavior and crystal growth mechanism of erythromycin in aqueous acetone solution

Zhanzhong Wang†, Wenzhi Fang, and Yan Li

School of Chemical Engineering and Technology, Tianjin University, Tianjin 300072, P. R. China
(*Received 30 May 2013 • accepted 4 October 2013*)

Abstract−The solubility of erythromycin acetone solvate and dihydrate was experimentally determined in aqueous acetone mixtures at different temperature. It has been demonstrated that solubility curves of the two solvates intersected at given solvent composition at various temperature, suggesting a transition behavior between two solvates. The induction period of acetone solvate at different supersaturation was measured by the laser monitoring observation technique. Based on classical homogeneous nucleation theory, the solid-liquid interfacial tension and surface entropy factor were calculated from the induction period data. From the surface entropy factor values calculated, together with surface morphology observation by the atomic force microscopy (AFM), the growth mechanism of erythromycin acetone solvate is consistent with continuous growth mode.

Keywords: Erythromycin, Crystal Growth Mechanism, Solvated Crystals, Induction Time, Transformation

INTRODUCTION

Polymorphs and pseudopolymorphs, which are also called solvated crystals, are a kind of phenomenon which is related to the crystalline solid state. Polymorphs are compounds resulting from the possibility of at least two different arrangements of the molecules, leading to have different lattice type between a crystal form and another one. Pseudopolymorphs are crystals formed by the same substance crystallized with different amounts of types of solvent molecules. So pseudopolymorphs not only have their molecules arranged differently but also normally have a significantly different molecular composition [1]. Polymorphs and pseudopolymorphs affect the bioavailability, stability, solubility, and morphology of crystal products such as pharmaceuticals. Controlling polymorphism and pseudopolymorphism is of great interest in fields such as solid-state chemistry, materials science, pharmacology, and other applications [2]. Their crystallization behavior is composed of the competitive nucleation, growth, and transformation from a metastable form to a stable form. To selectively crystallize specific crystal form, the mechanism of each elementary step in the crystallization process with regard to the operational conditions needs to be elucidated [3].

Erythromycin is a mixture of macrolide antibiotics produced by fermentation of strains of *Saccharopolyspora erythrea*. Treatment with this antibiotic drug in human and veterinary practice is still very common, because of the high activity against gram-positive and a few gram-negative strains [4]. Moreover, erythromycin is useful as an intermediate for the preparation of roxithromycin, azithromycin and clarithromycin. Erythromycin can form solvates with water or various organic solvents such as acetone, ethanol. Erythromycin A (Fig. 1) is the main and active component in erythromycin mixtures and commercial erythromycin is usually available as the dehydrate [5]. The traditional methods, such as varying solvent composition, temperature, supersaturation, and seeding strategy, have been extensively applied to control the polymorphic behavior of a pharmaceutical material during crystallization [6,7].

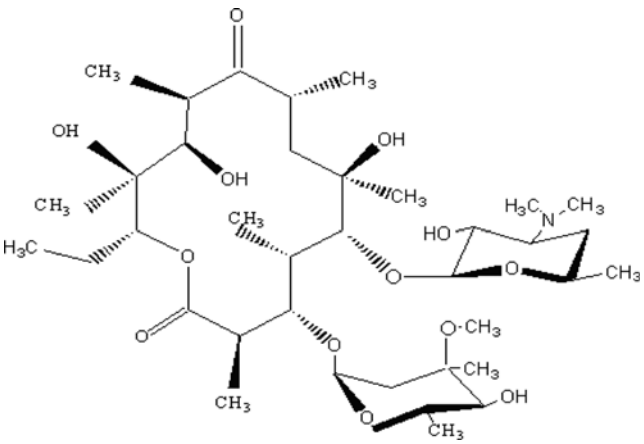

Fig. 1. Molecular structure of erythromycin A.

In experimental and industrial practice, acetone+water mixtures are often chosen as solvent system of erythromycin crystallization, and in this solvent system erythromycin can form two solvates during crystallization. Yoshinobu et al. [5] studied physical properties of erythromycin dihydrate, anhydrate and amorphous solid. Gregory et al. [8] made further solid-state investigations of erythromycin A dihydrate from aspects of structure, NMR spectroscopy, and hygroscopicity. Recently, Miroshnyk et al. [9] reported thermally induced phase transformation of erythromycin A dihydrate. Literature [10,11] survey indicates that investigations on erythromycin have received great attention. In a very recent study, we reported the solvent-mediated transformation of erythromycin solvates in acetone+water solvent system during antisolvent crystallization [12].

One of the characteristics of antisolvent crystallization is that the

†To whom correspondence should be addressed.
E-mail: wzz7698@tju.edu.cn

solvent composition varies as the process proceeds. It is possible that the solvent composition has an effect on not only the nucleation rate, but also transformation rate of polymorphs and pseudopolymorphs. Temperature is also an important factor influencing crystal growth. In addition, one important parameter of crystal nucleation kinetics is the period of time between the attainment of supersaturation and the formation of critical nuclei. This time, defined as induction time (t_{ind}), depends fundamentally on temperature and supersaturation. Induction time cannot be considered a fundamental property of the system. However, analysis of the values can help comprehension of mechanisms of new phase formation and growth from critical nuclei into crystals [13].

The interfacial tension plays a crucial role in the growth mechanism, which determines if two-dimensional nucleation is possible and dislocation is the only growth mode [14]. Therefore, determination of interfacial tension at different solvent composition and different temperature is important for studying the mechanism of crystal nucleation and growth. Atomic force microscopy (AFM) is a powerful tool to achieve information in relation with crystal growth mechanism. Since its invention in 1986, AFM has been widely used to study the growth mechanisms, the nanometer scale morphology of crystal surfaces [15].

In this paper, crystal growth mechanism of acetone solvate was investigated by measuring induction time to calculate interfacial tension and surface entropy factor. In addition, AFM was used to observe the surface morphology of crystals in nanometer scale. The transition behavior from acetone solvate to dihydrate is investigated from the aspects of phase equilibrium.

EXPERIMENTAL

1. Materials

Erythromycin A dihydrate (supplied from Xi'an Rejoy Co. Ltd., China, more than 99.0% in purity, Mw 769.94, molecular formula $C_{37}H_{67}NO_{13}\cdot 2H_2O$) was regarded as materials to carry out investigation. Acetone solvate was obtained by recrystallization of dihydrate. Acetone used for the experiments was of analytical reagent grade. Distilled deionized water of HPLC grade was used.

2. The Solubility of Erythromycin Solvates and Phase Transition Point

The solubility of each erythromycin solvate was measured with broader range than in the previous publication [12] in acetone+water mixtures at 35 °C, 40 °C, 45 °C, and 50 °C, respectively. Suspension samples withdrawn from the crystallizer were analyzed for the solid phase to verify the solid form present at equilibrium by microscope and XRPD (X-ray powder diffraction).

3. Measurement of the Induction Period for Acetone Solvate

The time at which the crystals were detected in the solution was noted as the induction time t_{ind}. Laser light scattering method [16] was used to measure induction time in this paper. The laser monitoring system was composed of a laser generator, a photoelectric transformer, and a light intensity display. The experiments were performed in a 50 mL, round-bottomed jacketed crystallizer. The crystallizer was equipped with a lid, a condenser and thermometer. The temperature of the crystallizer was controlled by a heat exchanger and programmable thermostatic batch (501A, China). Mixing was ensured by a magnetic force stirrer. For all the experiments, the stirring rate was taken equal to 250 rpm. Laser intensity change was used to help to detect the nucleation onset and to ensure that no residual solids were present at the beginning of the experiment.

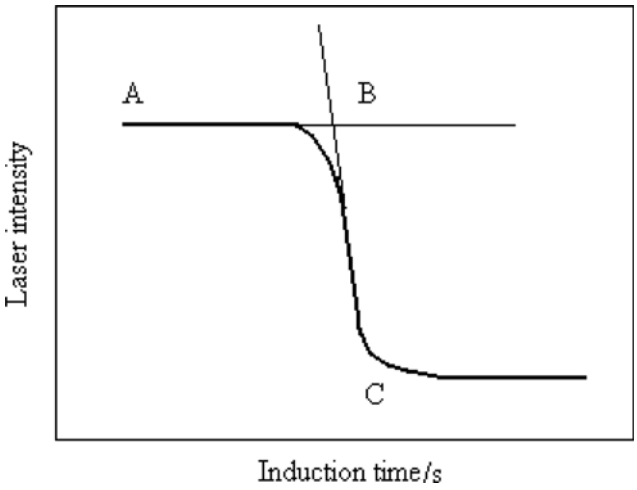

Fig. 2. Determination sketch of the nucleation induction time by means of the laser method.

Initially, a suspension of an amount of acetone solvate in aqueous acetone solution with given solvent composition was heated 3 °C above the equilibrium temperature under agitation to dissolve all crystals for at least 30 min. It was then filtered through a 0.2 μm membrane filter. The solution filtered was added to the crystallizer, the temperature of which was kept within ±0.02 °C of the desired value. The laser monitoring system was turned on. An amount of water of desired temperature value was quickly added. Laser intensity was kept constant as shown in point A of Fig. 2. As nucleation started, the intensity of the laser beam penetrating the vessel dramatically dropped to the minimum as shown point C in Fig. 2. The time in the measurement was recorded. A change between the laser intensity data and the time was correlated. A typical measurement of the nucleation of supersaturated solution can be found at point B in Fig. 2. Induction time was figured out by the time from point A to point B.

Experiments under each set of conditions, defined by supersaturation ratio S and nucleation temperature T, were reproduced three times. The supersaturation ratio was calculated as $S=c/c_{eq}$, where c and c_{eq} are the initial concentration of acetone solvate and the equilibrium solubility at nucleation temperature T of the solid phase appearing in the experiment, respectively. The reported induction time, t_{ind}, is the average of reproducible measurements. The uncertainty is smaller than 5%.

4. The Atomic Force Microscopy (AFM) Measurement for Surface Morphology of Acetone Solvate

Acetone solvate was crystallized by adding water to dissolved dihydrate in the acetone. Crystal samples used here were grown by antisolvent crystallization method of adding water to acetone at 35 °C. A transparent, well-developed and needle-like crystal was used. The crystal surfaces for observation were obtained by gently pressing freshly selected crystals. The crystal surfaces in parallel with the glass plate were measured by a MMAFM/STM+D3100 atomic force microscope (AFM, made in America) equipped with a microcantilever (20 mm in length and 0.02 N/m in spring constant). A

glass plate with a crystal fixed on it was mounted on a stainless steel plate. The sample crystal was placed in the space between the stainless steel plate and cantilever holder. The crystal were scanned in contact mode using a standard program supplied by the manufacturer with a scan size 2×2 μm, a scan height 20 nm and a scan rate 3.052 Hz. The image was observed by an Olympus optical microscope attached to the AFM.

5. X-ray Powder Diffraction (XRPD) and Scanning Electronic Microscopy (SEM)

X-ray powder diffraction experiments were performed using X-ray powder diffraction (D/MAX 2500 Japan) with Cu Kα radiation of wavelength 1.5406 Å at 200 mA and 40 kV. The sample was packed into a plastic holder and was scanned from 3° to 40° 2θ at a step size 0.02° with a dwell time 1 s. Divergence slits and receiving slits were 1° and 0.15 mm, respectively. The crystal morphology of erythromycin solvates was also observed taking advantage of scanning electronic microscopy (JSM-6700F, Japan).

RESULTS AND DISCUSSION

1. Solubility Erythromycin Solvates

The thermodynamic stability and transformation behavior of polymorphs and solvates were examined in relation with the solubility in each crystal [17]. According to determined solubility of erythromycin solvates in acetone+water mixtures from 35 °C to 50 °C, the typical solubility curves of two solvates at 35 °C was plotted in Fig. 3. In Fig. 3, the solubility curves of both solvates approximately cross at water mass fraction 0.73, which is assumed to be the phase transition point of two solvates. Solubility of dihydrate is higher than that of acetone solvate at the left of the transition point and acetone solvate is the stable form. At the right of transition point, the case is the reverse. Solubility of acetone solvate is higher than that of dihydrate and dihydrate is the stable form.

Corresponding to 35 °C, 40 °C, 45 °C, 50 °C, the solubility curves of both solvates approximately cross at water mass fraction 0.73, 0.79, 0.84, and 0.86 in binary solvents, respectively. Change at solvent composition of phase transition point with temperature is plotted in Fig. 4. It is evidence that there is a tendency of phase transition point transferring to the side of high water content with an increase in the temperature. From Fig. 3 and Fig. 4, it is concluded that the thermodynamic stability between acetone solvate and dihydrate is sensitively influenced by solvent composition and temperature. Morphology and XRPD patterns of both erythromycin solvates are shown in Fig. 5. The difference in the crystal morphology between erythromycin acetone solvate and erythromycin dihydrate is obviously recognized. The crystal morphology of erythromycin acetone solvate is needle-like, whereas that of erythromycin dihydrate is plate-like as shown Fig. 5.

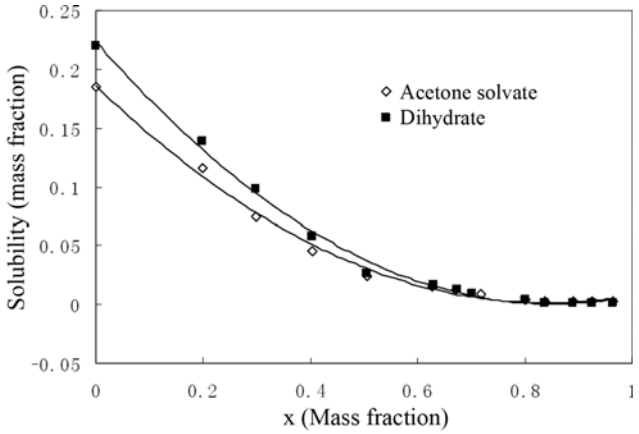

Fig. 3. Measured solubilities of erythromycin solvates in aqueous acetone solution at 35 °C.

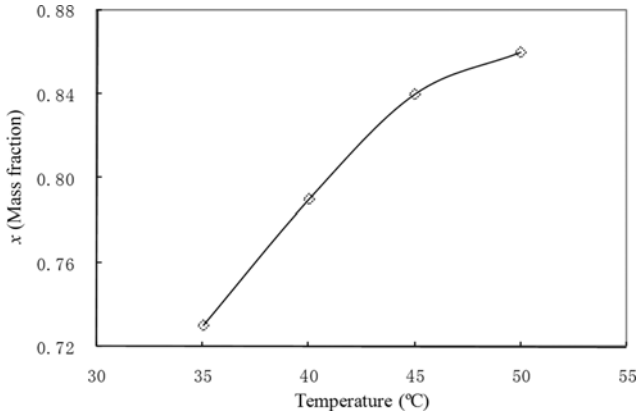

Fig. 4. Change of solvent composition at phase transition point with temperature.

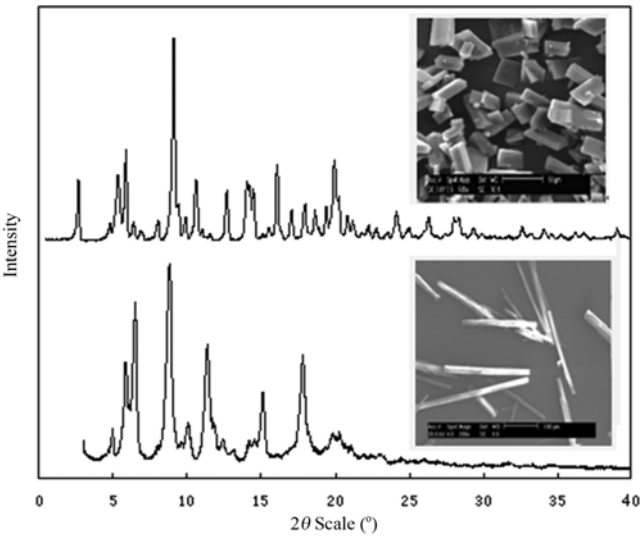

Fig. 5. Erythromycin acetone solvate (down) and dihydrate (up) crystal images by SEM and XRPD measurement.

2. Induction Time and Interfacial Tension

For homogeneous nucleation, the nucleation rate can be expressed as [18]

$$J_p = B\exp\left[-\frac{16\pi\gamma^3 V_m^2}{3v^2k^3T^3\ln^2 S}\right] \quad (1)$$

where J_p is the nucleation rate, k is the Boltzmann constant, T is the absolute temperature, S is the supersaturation ratio; v is the number of ions into which a solute molecule dissociates (1 for erythromycin molecule), γ is the crystal-solution interfacial tension and V_m is the volume of molecule. Eq. (1) is the classical rate equation for homogeneous nucleation. The nucleation rate is inversely pro-

portional to the induction time [14].

$$t_{ind}^{-1} \propto J_p \tag{2}$$

According to Eq. (1) and Eq. (2), the relationship between induction period and supersaturation can be represented as

$$\ln t_{ind} = K + A\frac{1}{\ln^2 S} \tag{3}$$

This suggests a straight line for $\ln t_{ind}$ against $1/\ln^2 S$ with the slope given by

$$A = \frac{16\pi\gamma^3 V_m^2}{3v^2 k^3 T^3} \tag{4}$$

So interfacial tension at the given solvent composition and temperature can be calculated from Eq. (3) and Eq. (4). The interfacial tension is a basic parameter for the determination of growth mechanism. There are three categories for crystal growth: continuous growth mode, surface nucleation mode and spiral growth mode. Surface entropy factor α is a measure of the roughness degree of the crystal surface. Increase of α means the crystal surface becomes smoother and crystal growth becomes more difficult [11]. For the real solution growth system, Davey suggested that surface entropy factor α could be calculated by using interfacial tension data [19].

$$\alpha = \frac{4V_m^{2/3}\gamma}{kT} \tag{5}$$

For α<2.0 it is expected that the interface will be rough and continuous growth will occur. When α>5.0, the interface becomes so smooth that screw dislocation or spiral growth will dominate. When α=2.0 to 5.0, birth and spread growth or two-dimensional nucleation is to be expected. Therefore, from the α value, the crystal growth mechanism can be estimated. The plots of t_{ind} against S at the temperature of 30 to 45 °C in different supersaturation are illustrated Fig. 6. From Fig. 6, initial supersaturation is critical to nucleation and induction time t_{ind} decreases with increase of supersaturation level. The temperature also has an obvious effect on the induction period. At constant supersaturation, the induction period tends to become short with increase of temperature, which implies that the formation of primary nuclei is more and more difficult with decrease

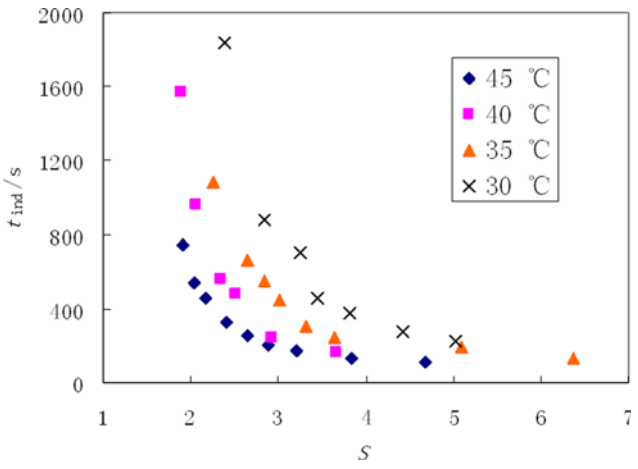

Fig. 6. t_{ind} against *S* for EMAS at different temperature.

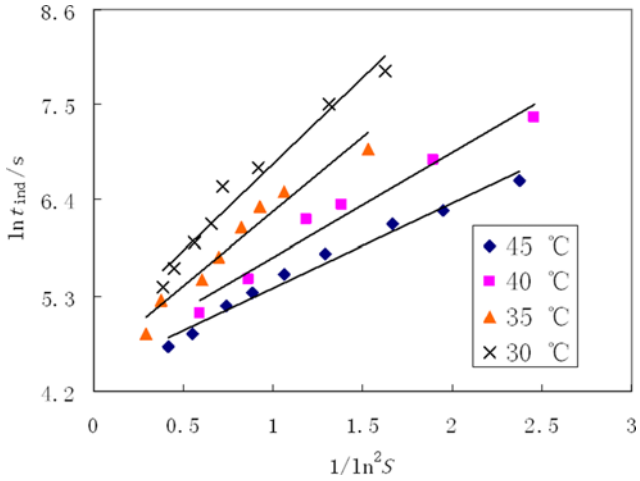

Fig. 7. $\ln t_{ind}$ against $1/\ln^2 S$ for EMAS at different temperature.

Table 1. Calculated values of interfacial tension (γ), surface entropy factor (α) and regression factor (R)

T/K	$\gamma \times 10^3$/(J/m^2)	α	R
303.00	2.03	2.12	0.9832
308.00	1.95	2.01	0.9782
313.00	1.82	1.84	0.9842
318.00	1.69	1.67	0.9900

of temperature in the process of cooling. In other words, the erythromycin solution will keep the metastable state for an even longer time as the temperature decreases.

The relation between induction time and supersaturation is also presented by $\ln(t_{ind})$ against $1/(\ln^2 S)$ in Fig. 7. Interfacial tension can be calculated from the slope of the straight line regressed by $\ln(t_{ind})$ and $1/(\ln^2 S)$ data. Calculated interfacial tensions and regression factors are listed in Table 1. From Table 1, the interfacial tension obtained is in the range from 1.69 to 2.03 kJ/m^2. The interfacial tension decreases with increase of temperature, which means nucleation becomes easier and easier with increase of temperature.

3. Crystal Growth Mechanism for Acetone Solvate

According to Eq. (5), combined with calculated interfacial tension, surface entropy factor α values are obtained and also listed in Table 1. The confidence level of the results is all above 95%. The uncertainty is mainly from the time lag of the measuring technique. From Table 1, surface entropy factor values decrease from 2.12 to 1.67 with increase of temperature from 30 °C to 45 °C. This result means that the energy barrier for growth of acetone solvate in acetone +water mixtures is relatively low and the crystal nuclei of acetone solvate grow continuously, from which can be assumed that the crystal surface of acetone solvate is rough and the growth rate of crystal is supposed to be fast. When crystallization temperature is at 30 °C, the energy barrier for crystal growth becomes big, and the surface entropy factor is beyond 2.0. In this case, the crystal growth turns to be controlled by birth and spread and the crystal surface can become smoother. As a powerful tool, the AFM was applied to achieve information in relation with crystal growth mechanism. In this paper the crystal faces parallel to the longest aspect of the EMAS needle were investigated using AFM. The AFM image of crystal surface

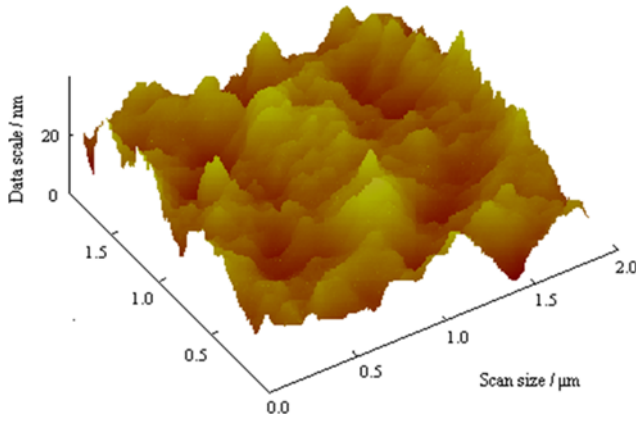

Fig. 8. Surface morphology for EMAS crystals by AFM measurement.

of acetone solvate is shown in Fig. 8. According to AFM measurement, a rough crystal surface in nanometer scale is observed. This feather is different from surface nucleation and spiral growth mode. Thus it is further confirmed that crystal growth of acetone solvate is in agreement with continuous growth mode.

CONCLUSIONS

The solubility of erythromycin over a temperature range from 35 to 50 °C has been determined in aqueous acetone mixtures by measuring the solute concentrations in equilibrated liquid solutions. The solubility values decrease with increase of water content in binary mixtures. For each temperature, the experiments determined specific solvent composition at which there was a transition from the acetone solvate form to the dihydrate form. The acetone content in mixed solvents at the transition point varied inversely with temperature. According to the induction time measured, interfacial tension and surface entropy factor were calculated. They all decreased with increase of temperature. Thus, crystal growth of acetone solvate can benefit from a proper increase of temperature during crystallization. Based on surface entropy factor calculated, together with crystal surface observation from the AFM, the growth mechanism of erythromycin acetone solvate is in agreement with continuous growth mode.

REFERENCES

1. A. Nangia, *Cryst. Growth Des.*, **6**, 2 (2006).
2. D. Chopra and T. N. Guru Row, *Cryst. Growth Des.*, **7**, 848 (2007).
3. M. Kitamura, *Cryst. Growth Des.*, **4**, 1153 (2004).
4. G. Cindy, K. C. Hezekiah and V. S. Ann, *Rapid Commun. Mass Sp*, **14**, 878 (2000).
5. F. Yoshinobu, F. Yomoaki and Y. Yuko, *Chem. Pharm. Bull.*, **31**, 4029 (1983).
6. G. Madrasa and B. J. McCoy, *Chem. Eng. Sci.*, **59**, 2573 (2004).
7. M. Kitamura and S. Hironaka, *Cryst. Growth Des.*, **6**, 1214 (2006).
8. A. S. Gregory, G. S. Joseph and H. P. Stowell, *J. Pharm. Sci.*, **86**, 1239 (1997).
9. I. Miroshnyk, L. Khriachtchev and S. Mirza, *Cryst. Growth Des.*, **6**, 369 (2006).
10. M. N. Butler and W. J. Weber, *Environ. Sci. Technol.*, **39**, 2301 (2005).
11. A. E. Graham, A. V. Thomas and R. Yang, *J. Org. Chem.*, **65**, 2583 (2000).
12. Z. Z. Wang, J. K. Wang and L. P. Dang, *Ind. Eng. Chem. Res.*, **46**, 1851 (2007).
13. A. Bernardo, C. E. Calmanovici and E. A. Miranda, *Cryst. Growth Des.*, **4**, 799 (2004).
14. H. X. Hao and J. K. Wang, *J. Cryst. Growth*, **274**, 545 (2005).
15. Y. L. Geng, D. Xu and X. Q. Wang, *J. Cryst. Growth*, **280**, 266 (2005).
16. A. Lancia, D. Musmarra and M. Prisciandaro, *AIChE J.*, **45**, 390 (1999).
17. M. Kitamura and K. Nakamura, *J. Cryst. Growth*, **236**, 676 (2002).
18. K. Selvaraju, R. Valluvan and S. Kumararaman, *Mater. Lett.*, **60**, 1549 (2006).
19. R. J. Davey, *Curr. Topics Mater. Sci.*, **8**, 454 (1982).